 https://doi.org/10.1051/e3sconf/202672004001

Electromagnetic actuator based in potential energy harnessing for highly dynamic applications

Diego Lopez-Pascual[1*], *Oscar* Manzano-Narro[2], *Miguel* Albertos-Cabanas[2], *Miguel* Fernandez-Munoz[2], *Hugo* Rodriguez-Bodoque[2], *Ignacio* Valiente-Blanco[2] and *Efren* Diez-Jimenez[2].

[1]Universidad de Alcalá, Escuela Politécnica Superior, Dpto. Teoría de la Señal y Comunicaciones, Área de Ingeniería Eléctrica, Ctra. Madrid-Barcelona km 33.6, Alcalá de Henares, España.
[2]Universidad de Alcalá, Escuela Politécnica Superior, Dpto. Teoría de la Señal y Comunicaciones, Área de Ingeniería Mecánica, Ctra. Madrid-Barcelona km 33.6, Alcalá de Henares, España.

Abstract. Conventional electromagnetic actuators' energy consumption is largely determined by the need to accelerate and decelerate the driven payload, with stricter switching time requirements and heavier loads leading to higher power demands. These devices are ubiquitous across most industries, and thus increasing the efficiency of such actuators is therefore a key objective. Within this context, a novel rotary electromagnetic actuator for ultra-low-power positioning was developed and experimentally validated. The device operates by harnessing the magnetic potential energy stored between permanent magnets arranged with opposing magnetization directions. Combined with active electromagnetic control and a passive stabilization system, the actuator's rotor switches between stable equilibrium positions rapidly (in the order of tens of miliseconds) and with significantly reduced power consumption compared to conventional electromagnetic actuators. Experimental tests were carried for the device for both dynamic and quasi-static operation, which confirmed the theoretical predictions. The results demonstrated a torque of 590 mNm with a peak power consumption of only 6.3 W. The total energy consumption was measured at 180 J. These results represent an 80% reduction in peak power consumption relative to a conventional electromagnetic actuator, validating the effectiveness of the proposed design under real operating conditions.

1 Introduction

High-precision and rapid linear or angular positioning of a payload is essential in numerous engineering and scientific applications. Representative examples of common applications include process-feeding systems, serial manufacturing and tool-change mechanisms for machining centers [1], robotic manipulators [2], [3], biomedical devices [4], [5], rotary indexing tables [6], and optical filter wheels employed in advanced instrumentation [7]. In all these systems, the payload must undergo rapid acceleration followed by controlled

* Corresponding author: d.lopezp@uah.es

deceleration to reach commanded positions both quickly and accurately. As a result, the power demanded by the associated actuators increases sharply with the required acceleration, leading to significant growth in overall energy consumption.

Moreover, the high-power demand typically forces actuation systems and power electronics to be oversized in terms of mass and volume, while heat dissipation becomes a major design constraint. These issues often compromise the feasibility of conventional electromagnetic actuators [8]–[10] and contribute to elevated environmental impact and operational costs [11]. Within this context, achieving high torque density, high rotational speed, and minimal power consumption represents a significant engineering challenge and a critical performance requirement.

This paper introduces a novel electromagnetic actuator based on the concept of harnessing of potential magnetic energy, which was previously explored theoretically in a previous paper [12]. The proposed approach represents a substantial advancement in electromagnetic actuation for highly dynamic positioning applications in which minimizing power and energy consumption is paramount. A theoretical description of the magnetic-energy-harvesting principle is presented, followed by the development and experimental evaluation of a prototype actuator designed for driving an optical filter-wheel payload. The results validate the underlying actuation principle and demonstrate its strong potential to deliver substantial reductions in both power demand and energy usage for these classes of systems.

2 Prototype description and working principle

The actuator incorporates permanent magnets in both the rotor and stator arranged magnetized parallel to the axis of rotation and with opposing magnetization directions. When aligned at one of the discrete equilibrium positions, magnetic repulsion stores potential energy. Stabilization fins made of soft magnetic materials generate localized potential wells that convert otherwise unstable equilibrium points into stable ones. This effect can be observed in Fig. 1. Motion between successive equilibrium positions is achieved by energizing axial coils mounted on the stator that overcome the stabilization torque, allowing the stored magnetic energy to be released and transformed into kinetic energy. As a result, only a small fraction of the energy normally required for acceleration and braking must be supplied electrically.

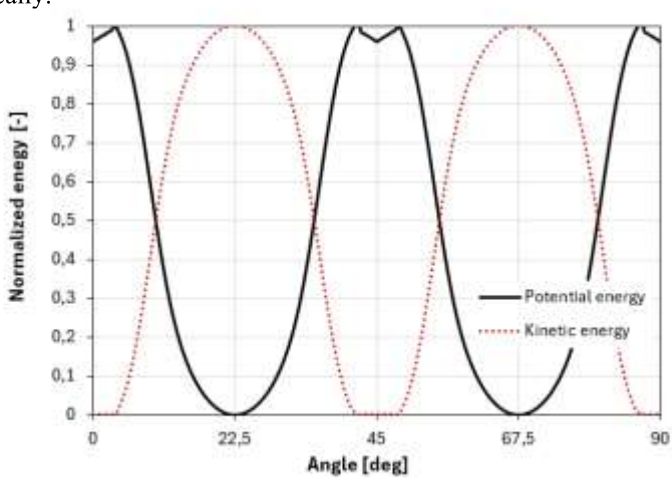

Fig. 1. Kinetic and potential energy of the rotor (normalized) vs position.

A prototype actuator (shown in Fig. 2.a) of 86 mm diameter and 25 mm thickness was fabricated and instrumented for performance characterization. The rotor, which includes 16

NdFeBr N35H permanent magnets, has a moment of inertia of 3.5×10^{-5} kg·m². These magnets have a size of 3x3x10 mm and are mounted in two concentric sets of 8 with opposite magnetization directions. The finished rotor is shown in Fig. 2.b. Additionally, the stator is formed by two symmetrical yokes built from AISI 1020. One of these two yokes can be observed in Fig. 2.c. Each of these contain 8 PMs identical to those on the rotor, and with opposite magnetization direction to the magnets in the interior section of the rotor. Additionally, each yoke also presents 8 stabilization fins, which measure 13.1 mm in length, and 1 mm in thickness. These are used to generate the stabilization positions. A series of 8 coils on each side of the stator, are connected in anti-series to the next one, with both sets of coils connected in series. The total measured resistance of the coils is 25.4 Ω and their inductance 14 mH. Two NSK bearings with a 24.1 mm outer diameter complete the assembly.

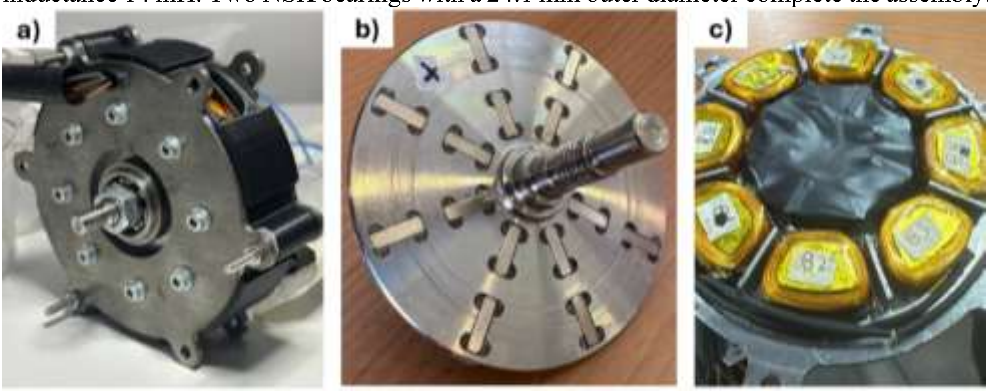

Fig. 2. Pictures of the assembled actuator (a), rotor (b), and one of the yokes that form the stator (c)

3 Experimental set-up and test procedure

Two different test setups were built for the operational characterization of the actuator (1). First, quasi-static torque measurements were performed using a 1Nm Lorenz torque sensor (2) and a Sick optical encoder with 4 arcmin resolution (3). A geared NEMA 17 bipolar stepper motor (4), with 20 Nm maximum torque, was used to rotate the actuator, and thus measure the experienced torque vs angular position. This setup can be observed in Fig 3.a. With this setup, the torque curve of the actuator can be obtained, and it is presented in the following section of the paper. Then, a second setup is constructed for dynamic testing, with which angular motion, acceleration, and energy consumption are evaluated. This setup uses the same angular encoder, but does not require any motor or torque sensor, since the movement is generated by powering the actuator itself. By providing a very short electrical pulse, the motor is taken out of its stable position, and its position shifts to the next stable position. Switching times are precisely measured, and from those, mechanical power output is determined. Dynamic tests were executed both with and without a representative filter-wheel payload (5), as can be observed in Fig 3.b. Data acquisition was performed using a National Instruments NI USB-6211 16-bit A/D board, which was also employed for actuator control. A Korad KD-3305D adjustable DC power supply provided the input voltage and current to the motor. The input current was measured by monitoring the voltage drop across a precision 0.25 Ω resistor placed in series with the actuator winding.

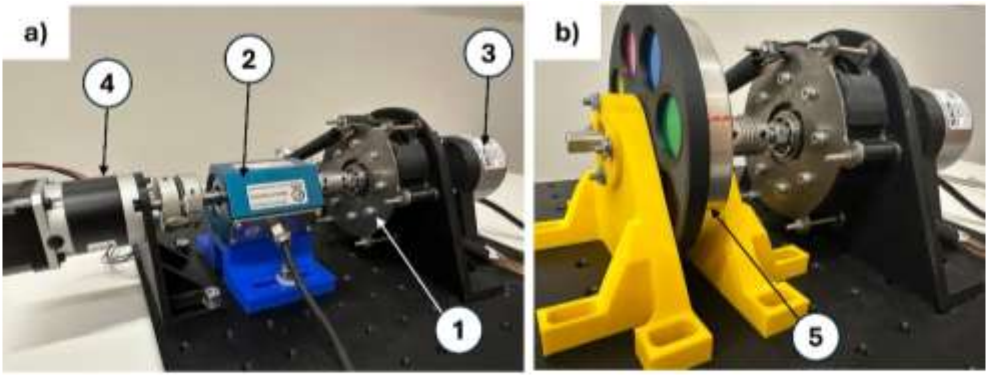

Fig. 3. Quasi-static (a) and dynamic (b) test setups for the actuator.

4 Experimental results

4.1 Torque measurements

Fig. 4 compares quasi-static torque–angle measurements without an input current with the finite element model (FEM) results reported in the previous paper [12]. The experimental data show strong agreement with simulations. When no current flows through the coils, the actuation torque is measured in 536±6 mNm. When a 500 mA current is circulated through the coils, this torque increases to 590±6 mNm. The mean absolute value of the maximum and minimum stabilization torque around the stable positions was measured to be 7±2 mNm.

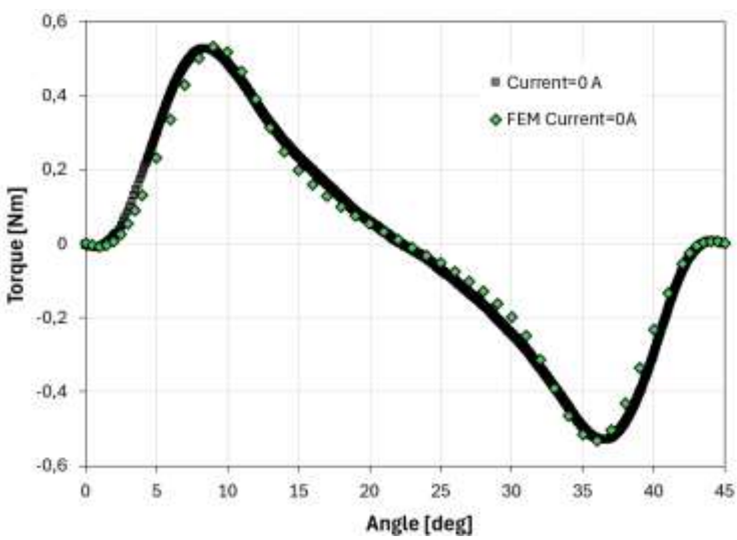

Fig. 4. Torque vs. angle between two stable positions. Experimental measurement vs FEM simulation presented in [12].

https://doi.org/10.1051/e3sconf/202672004001

4.2 Dynamic performance

Dynamic characterization was first performed for transitions between the 0° and 45° stable positions, both with and without payload. The actuator was driven using an excitation voltage of approximately ±12.7V, producing a peak current of ±500mA, the minimum required for reliable switching.

Fig. 5 shows the rotor angle over time during a position switch for both inertia configurations. From these data, maximum angular speeds of 663 rpm ($\eta_J = 1.1$) and 216 rpm ($\eta_J = 11$) are obtained, with corresponding peak angular accelerations of 1.45×10^4 rad/s^2 and 1.54×10^3 rad/s^2, respectively. The time required to step between adjacent equilibrium positions is *t1* = 48 ms without payload and *t2* = 140 ms with payload. As expected, increasing system inertia reduces acceleration and speed, thereby increasing transition time.

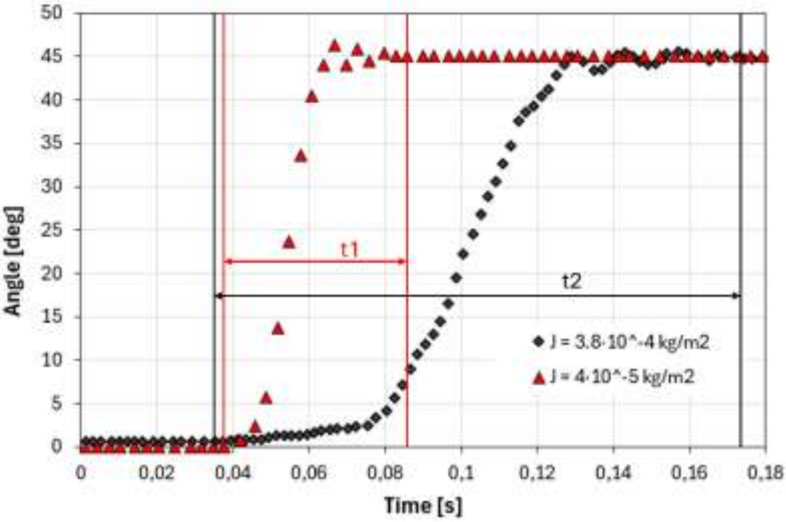

Fig. 5. Angular position of the rotor over time while performing a position change for different inertia configurations.

4.3 Power and Energy consumption

A major objective of the study is to quantify the potential of the proposed actuator for power and energy reduction in dynamic applications, and compare it with conventional electromagnetic actuators performance. The measured electrical power and energy consumption are then compared with those of a conventional electromagnetic actuator capable of producing the same motion. The maximum electrical power consumption of the proposed actuator is 6.3 W, independent of payload. Equivalent power requirements for a conventional actuator are evaluated based on the mechanical power output achieved by the presented actuator. Friction torque (experimentally measured between 0 and 750 rpm) remains approximately constant at 10 mNm with or without the payload. Electromagnetic losses, obtained through FEM in [12], are incorporated into the power model, while secondary loss sources such as bearing friction and misalignment are neglected.

Fig 6 compares the equivalent conventional actuator power (calculated for an ideal conventional electromagnetic actuator with 100% efficiency) with the experimentally measured power consumption of the proposed device. From this, the peak power saving ratio is calculated as 80% without payload and 40% with payload.

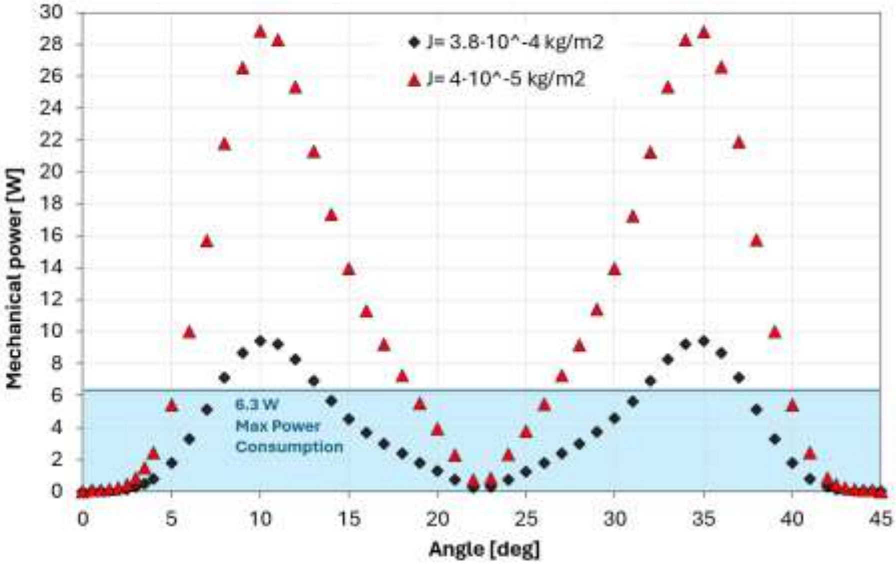

Fig. 6. Actuator's output power vs angle for both inertia configurations, compared with maximum measured power consumption.

5 Conclusions

In this paper, a novel type of electromagnetic actuator is presented. The prototype demonstrated high torque output (up to 590 mNm), fast switching between equilibrium states (as low as 48 ms), and consistent dynamic performance across different inertia configurations, while maintaining a peak power consumption of only 6.3 W and reducing equivalent power requirements by up to 80% compared to conventional electromagnetic actuators operating under the same conditions. These findings validate both the theoretical actuation principle and its practical feasibility, establishing the device as a compelling alternative for highly dynamic, energy-constrained applications. Future work may extend the approach to multi-step motion planning, more complex payloads, and integrated control architectures to further expand its applicability and performance envelope.

References

1. G. Gest, S. J. Culley, R. I. McIntosh, A. R. Mileham, and G. W. Owen, 'Review of fast tool change systems', Computer Integrated Manufacturing Systems, vol. 8, no. 3, pp. 205–210, Aug. 1995.
2. V. Vodovozov, Z. Raud, and E. Petlenkov, 'Intelligent Control of Robots with Minimal Power Consumption in Pick-and-Place Operations', Energies (Basel), vol. 16, no. 21, p. 7418, Nov. 2023.
3. B. Wei, 'Adaptive Control Design and Stability Analysis of Robotic Manipulators', Actuators, vol. 7, no. 4, p. 89, Dec. 2018.
4. Diez-Jimenez. E. and et al., 'Multilayered Microcoils for Microactuators and Characterization of Their Operational Limits in Body-Like Environments', IEEE/ASME TRANSACTIONS ON MECHATRONICS, 2022.
5. G. Villalba-Alumbreros, C. Moron-Alguacil, M. Fernandez-Munoz, I. Valiente-Blanco, and E. Diez-Jimenez, 'Scale Effects on Performance of BLDC Micromotors

for Internal Biomedical Applications: A Finite Element Analysis', J Med Device, vol. 16, no. 3, Sep. 2022.

6. O. Y. Taek, 'Design of precision angular indexing system for calibration of rotary tables', Journal of Mechanical Science and Technology, vol. 26, no. 3, pp. 847–855, Mar. 2012.
7. O. Krause et al., 'Cryogenic wheel mechanisms for the Mid-Infrared Instrument (MIRI) of the James Webb Space Telescope (JWST): detailed design and test results from the qualification program', Jul. 2008, p. 701824.
8. X. Ren, Z. Chen, R. Du, and M. Feng, 'Loss and Thermal Analysis of a High-Power-Density Permanent Magnet Starter/Generator', Energies (Basel), vol. 17, no. 20, p. 5049, Oct. 2024.
9. Z. Li et al., 'Loss calculation and thermal analysis of ultra-high speed permanent magnet motor', Heliyon, vol. 8, no. 11, p. e11350, Nov. 2022.
10. I. Valiente-Blanco, D. López-Pascual, M. A.-C. Nas, and E. Díez-Jiménez, 'Novel Method for the Characterization of the Electrical Conductivity and Eddy Current Damping of Aluminum Foams', IEEE Trans Instrum Meas, vol. 72, pp. 1–8, 2023.
11. K. J. Meessen, J. J. H. Paulides, and E. A. Lomonova, 'Analysis and design of a slotless tubular permanent magnet actuator for high acceleration applications', J Appl Phys, vol. 105, no. 7, p. 07F110, Apr. 2009.
12. M. Albertos-Cabanas, D. Lopez-Pascual, I. Valiente-Blanco, G. Villalba-Alumbreros, and M. Fernandez-Munoz, 'A Novel Ultra-Low Power Consumption Electromagnetic Actuator Based on Potential Magnetic Energy: Theoretical and Finite Element Analysis', Actuators, vol. 12, no. 2, p. 87, Feb. 2023.